

Template-Guided Sodium Intercalation Enables Phase-Pure Alkali Metal-based Ternary Chalcogenides Nanocrystals

Niraj Nitish Patil^{[1]}, Hannah McKeever^[1], Monika Ahlawat^[1], Kevin M Ryan^[1],
Shalini Singh^{[1]*}*

[1] Department of Chemical Sciences and Bernal Institute, University of Limerick, V94 T9PX
Limerick, Ireland

Table of Contents

1. Experimental Protocol.....	2
1.1 Reagents	2
1.2 Synthesis of NaIn ₃ Se ₅	2
1.3 Synthesis of NaInS ₂	3
1.4 Material Characterisation	3
2. Additional Characterisation	5
2.1 XRD analysis of NaIn ₃ Se ₅ NCs	5
2.2 Refinement Parameters for NaIn ₃ Se ₅ NCs.....	5
2.3 Surface characterisation for NaIn ₃ Se ₅ and NaInS ₂ NCs.....	6
2.4 Raman spectra of NaIn ₃ Se ₅ NCs	7
2.5 Control experiments	7
2.6 XRD analysis of NaIn ₃ Se ₅ NCs	9
2.7 Refinement parameters for NaInS ₂ NCs.....	10
2.8 FTIR spectra for NaInS ₂ NCs.....	10
2.9 Raman spectra for NaInS ₂ NCs	11
2.10 XRD, TEM and STEM-EDS analysis for In-S aliquot	11
2.11 Control experiments	12

1. Experimental Protocol

1.1 Reagents

Indium acetate, selenium powder, sulfur powder, sodium carbonate, octadecene (ODE, 90%), selenourea, diphenyldiselenide, diphenyldisulphide, 1-dodecanethiol (1-ddt), thiourea, oleylamine (OLA, 98%) and oleic acid (OA) were purchased from Sigma Aldrich. Toluene, isopropanol and ethanol were purchased from Lennonx, Ireland. The reagents were used as received without any further purification. To make 0.2 M sodium oleate (NaOL), 381.65 mg (3.6 mmol) of Na_2CO_3 was mixed with 30 ml of ODE and 4.5 ml of OA in a three-neck bottom flask (RBF), evacuated at 120 °C for 60 minutes, then heated to 150 °C under an Argon atmosphere for 3 hours.

1.2 Synthesis of NaIn_3Se_5

For the synthesis of NaIn_3Se_5 , 73 mg (0.25 mmol) indium acetate and 40 mg (0.5 mmol) Se powder were weighed into a RBF and suspended in 5 mL of OLA. The reaction mixture was placed under vacuum, heated to 120 °C over 5 minutes, and held under vacuum (> 200 mTorr) at this temperature for 30 minutes. After degassing, the system was purged with argon and heated to 260 °C. When the temperature reached 260 °C, 1.5 mL of Na-oleate was rapidly injected, and the reaction was allowed to proceed for a growth time of 150 minutes. The reaction was terminated by removing the heating mantle, and the solution was allowed to cool. At 80 °C, 10 mL of toluene was injected into the flask. The reaction mixture was transferred to a 50 mL centrifuge tube and vortexed. To precipitate the NCs, 10 mL of ethanol was added, followed by vortexing and centrifuging at 1000 RPM for 5 minutes. To wash the NCs, the precipitate was redispersed in 5 mL of toluene. A subsequent addition of 5 ml of IPA, followed by vortexing and centrifugation under the same conditions, was performed, and the supernatant was discarded. The precipitate was then subjected to two additional washing cycles with toluene/IPA using the same procedure. For reactions using different selenium precursors,

selenourea (0.5 mmol, 63 mg) and diphenyl diselenide (0.3 mmol, 93.6 mg) were each used in place of elemental Se, while all other reaction and purification conditions were kept unchanged. For temperature variation study Na-oleate was added at different temperatures (220 and 300 °C)

1.3 Synthesis of NaInS₂

The synthesis of NaInS₂ followed a protocol similar to that for NaIn₃Se₅. 29 mg (0.1 mmol) of indium acetate and 7 mg (0.2 mmol) of S powder were weighed out in a RBF and suspended in 5 mL of OLA. When the temperature reached 260 °C, 0.5 mL of Na-oleate was rapidly injected, and the reaction was allowed to proceed for a growth time of 60 minutes. For reactions using different sulfur precursors, thiourea (0.2 mmol, 15.2 mg), diphenyl disulfide (0.2 mmol, 43.2 mg) and 1-dodecanethiol {10 times more; (2 mmol, 400µL)} were each used in place of elemental S, while all other reaction and purification conditions were kept unchanged. For temperature variation study Na-oleate was added at different temperatures (180, 220 and 300 °C)

1.4 Material Characterisation

All XRD patterns were taken by drop-casting a film of the sample on a p-type boron-doped silicon zero background disk. The XRD experiments were conducted using a PANalytical Empyrean instrument equipped with a Cu K α radiation source ($\lambda = 1.5418 \text{ \AA}$) and a 1-D X'celerator strip detector with a diffractometer operating at 40 kV and 40 mA. TEM analysis was carried out by dispersing the samples in ethanol and drop-casting onto lacey carbon-coated 200-mesh nickel grids. High-resolution TEM (HRTEM) and high-angle annular dark-field scanning transmission electron microscopy (HAADF-STEM) were carried out using a 200 kV Talos F200i field emission microscope equipped with a Gatan UltraScan CCD camera and EDAX Genesis energy dispersive X-ray spectroscopy (EDS) detector. XPS spectra were measured using a Kratos AXIS ULTRA spectrometer fitted with a mono Al K α (1486.58eV)

X-ray gun. Calibration was performed using the C 1s line at 284.8 eV, while construction and peak fitting were performed using CasaXPS software. Samples for XPS analysis were prepared by drop-casting a film on a p-type boron-doped silicon wafer. UV-Vis-NIR spectroscopy was performed on a Cary 5000 spectrophotometer in 1 cm path-length cuvettes using toluene as the solvent. For the DRS measurements, powder samples were analysed using a Praying Mantis diffuse reflectance accessory attached to a Cary 5000 spectrophotometer. Raman spectroscopy was performed using a Horiba Labraman 300 spectrometer system equipped with a 620 nm laser.

2. Additional Characterisation

2.1 XRD analysis of NaIn_3Se_5 NCs

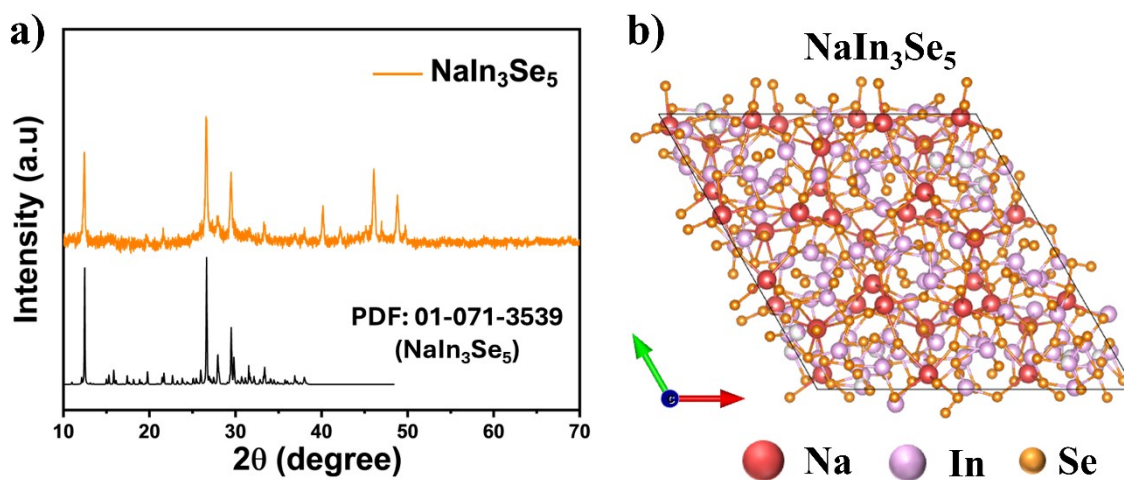


Figure S1 a) Indexed experimental XRD pattern, compared to a reference pattern of NaIn_3Se_5 with b) crystal structure.

2.2 Refinement Parameters for NaIn_3Se_5 NCs

Cell parameters	Experimental Values from Rietveld Refinement	Reference Pattern Values
a	24.582	24.570
b	24.582	24.570
c	17.427	17.414
α	90 °	90 °
β	90 °	90 °
γ	120 °	120 °

Figure S2 Refinement Parameters measured using Rietveld Refinement for NaIn_3Se_5 compared to the reference pattern values.

2.3 Surface characterisation for NaIn_3Se_5 and NaInS_2 NCs

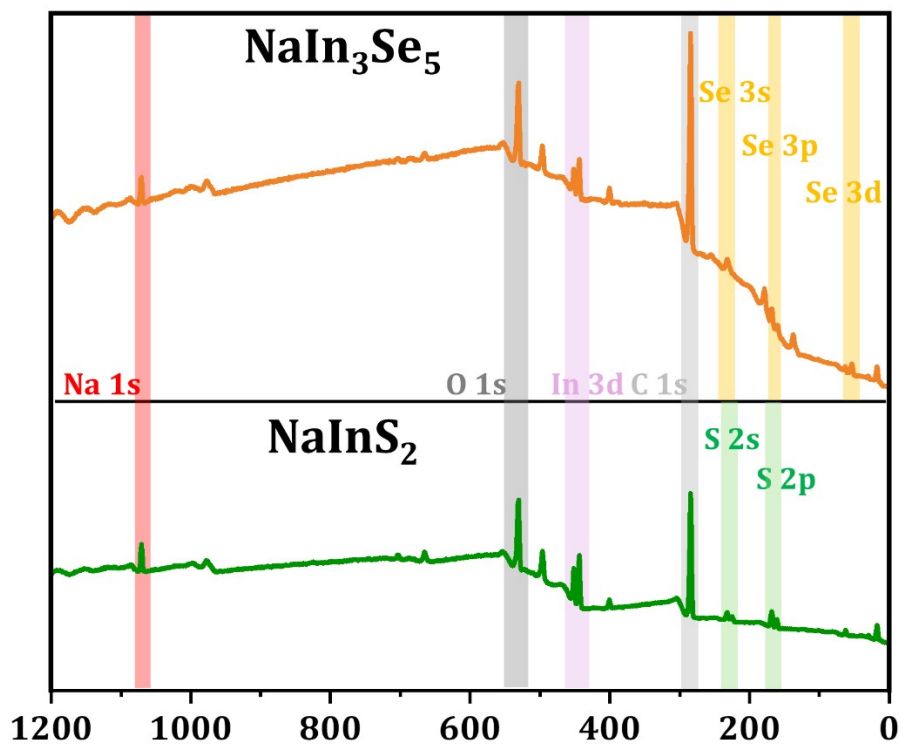


Figure S3 Full XPS Survey Spectra of NaIn_3Se_5 and NaInS_2 .

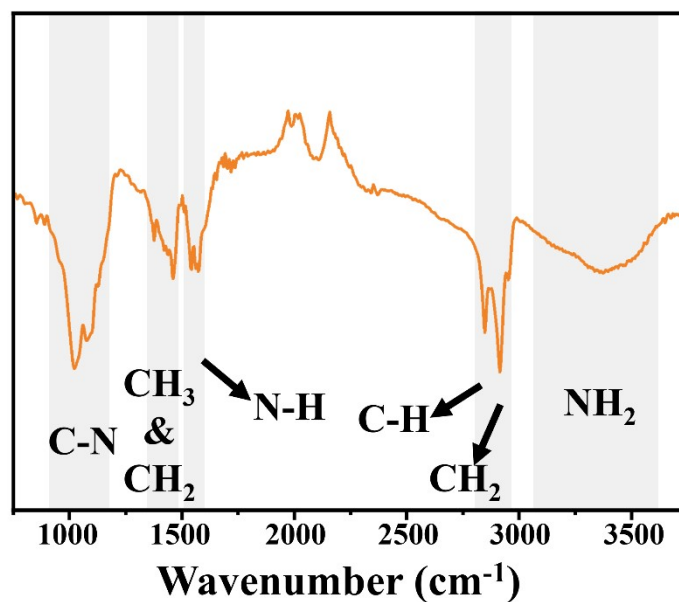


Figure S4 FTIR spectra of NaIn_3Se_5 NCs.

2.4 Raman spectra of NaIn_3Se_5 NCs

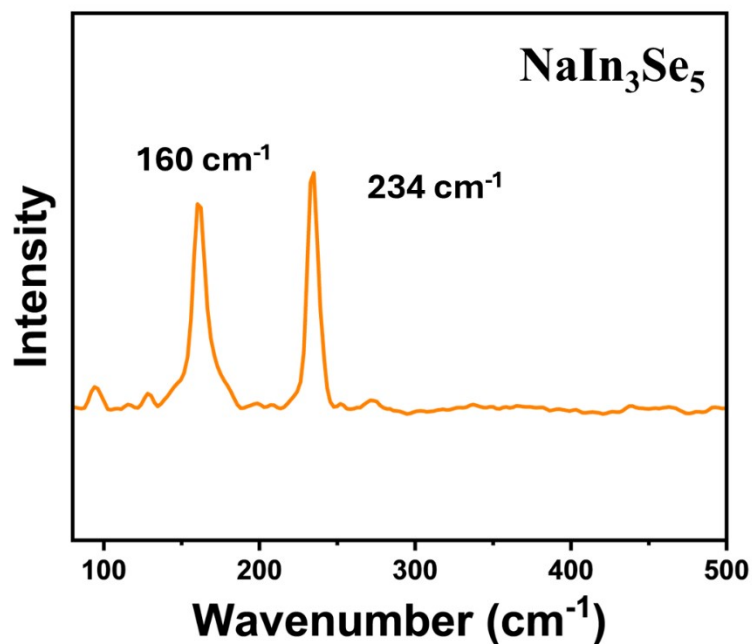


Figure S5 Raman spectra of NaIn_3Se_5 NCs.

2.5 Control experiments

2.5.1 Temperature variation study

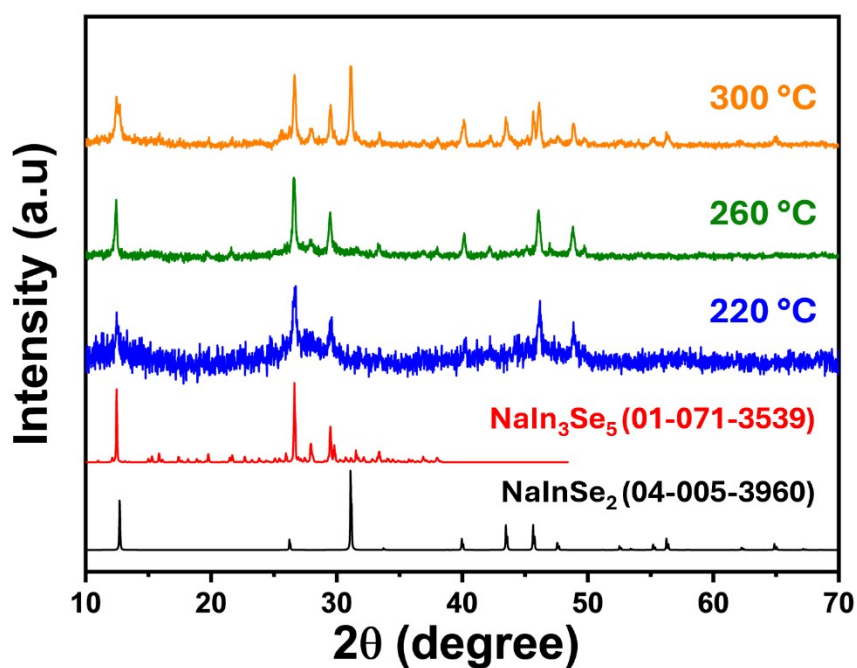


Figure S6 XRD patterns of Na-In-Se NCs synthesized by injecting Na-oleate at different temperatures.

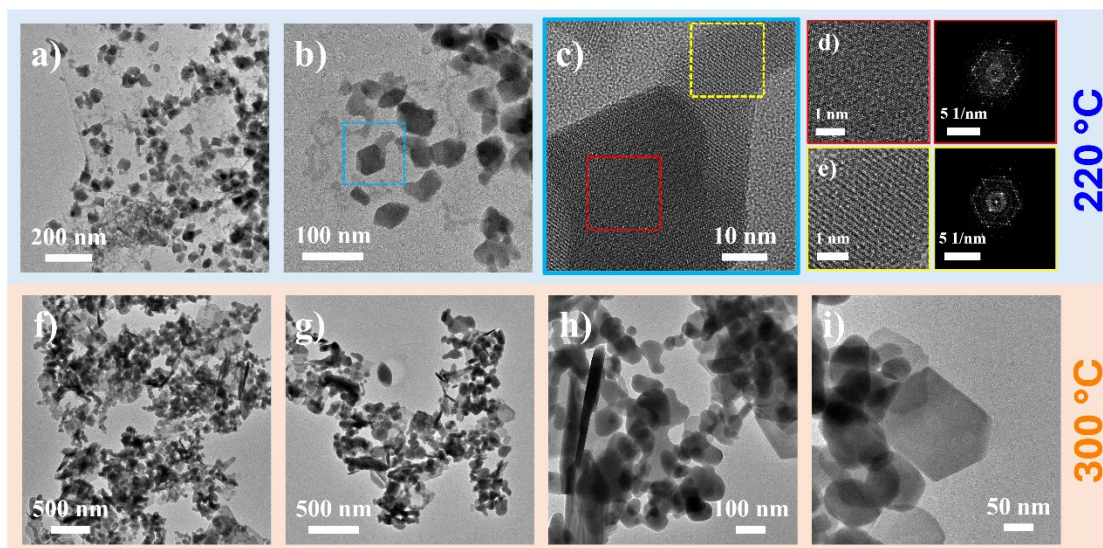


Figure S7 TEM images of Na-In-Se NCs synthesized by injecting Na-oleate at different temperatures.

2.5.2 Se source variation study

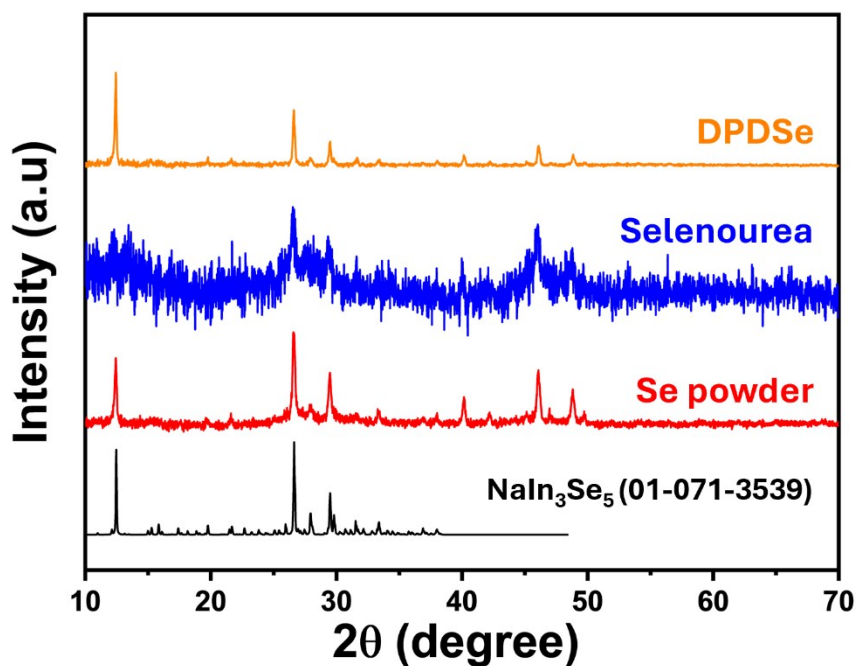


Figure S8 XRD patterns of Na-In-Se NCs synthesized by using different Se sources.

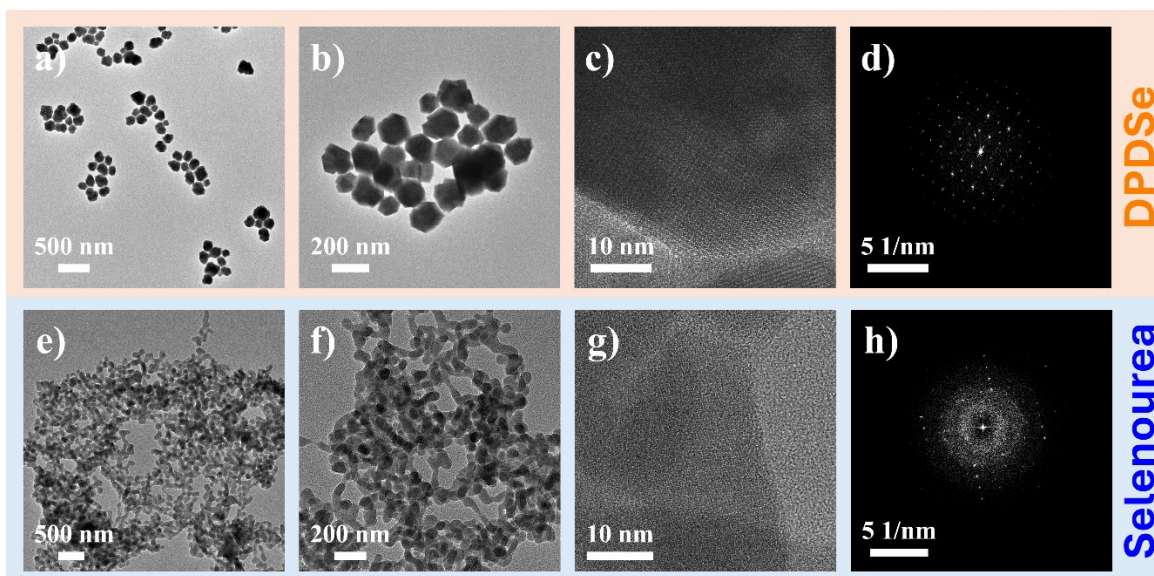


Figure S9 TEM images of Na-In-Se NCs synthesized by using different Se sources.

2.6 XRD analysis of NaIn_3Se_5 NCs

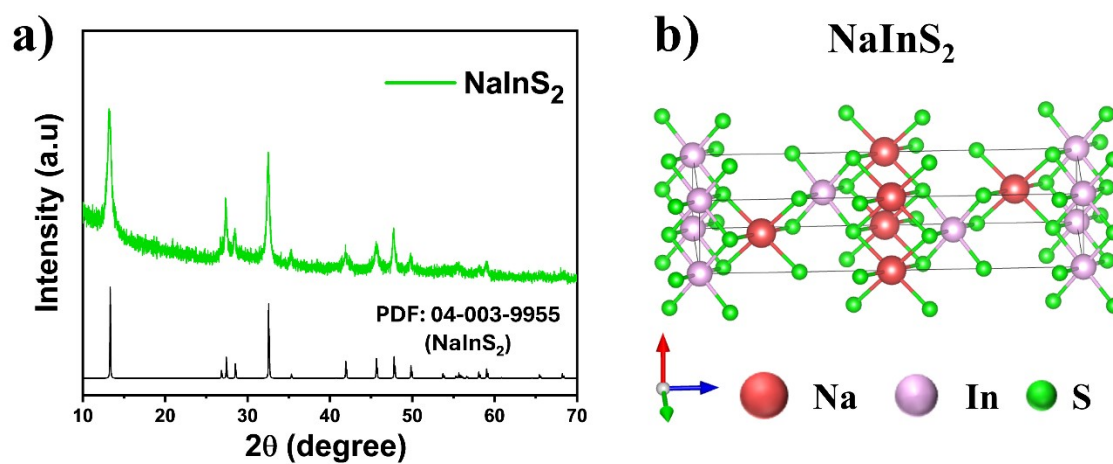


Figure S10 a) Indexed experimental XRD pattern, compared to a reference pattern of NaInS_2 with b) crystal structure.

2.7 Refinement parameters for NaInS₂ NCs

Cell parameters	Experimental Values from Rietveld Refinement	Reference Pattern Values
a	3.803	3.803
b	3.803	3.803
c	19.89	19.92
α	90 °	90 °
β	90 °	90 °
γ	120 °	120 °

Figure S11 Refinement Parameters measured using Rietveld Refinement for NaInS₂ compared to the reference pattern PDF No. 04-003-9955 values.

2.8 FTIR spectra for NaInS₂ NCs

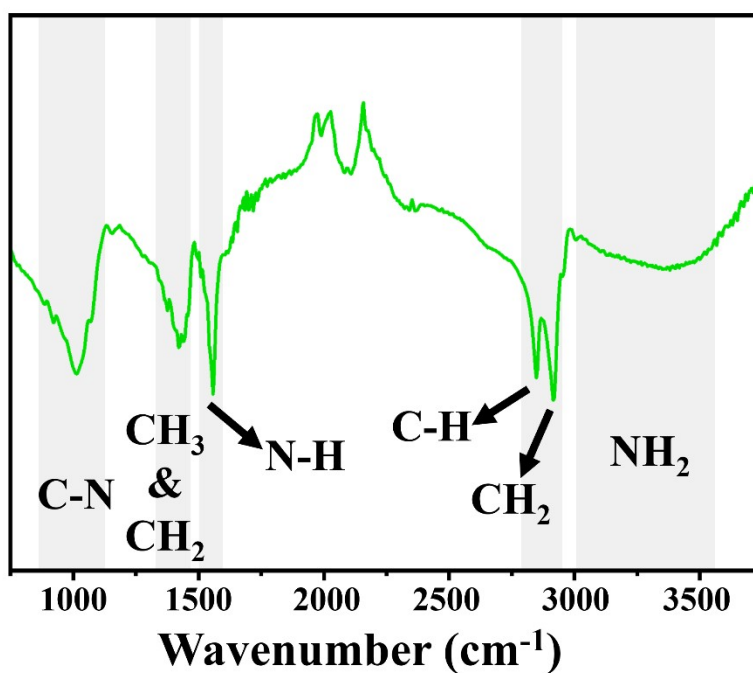


Figure S12 FTIR spectra of NaInS₂.

2.9 Raman spectra for NaInS₂ NCs

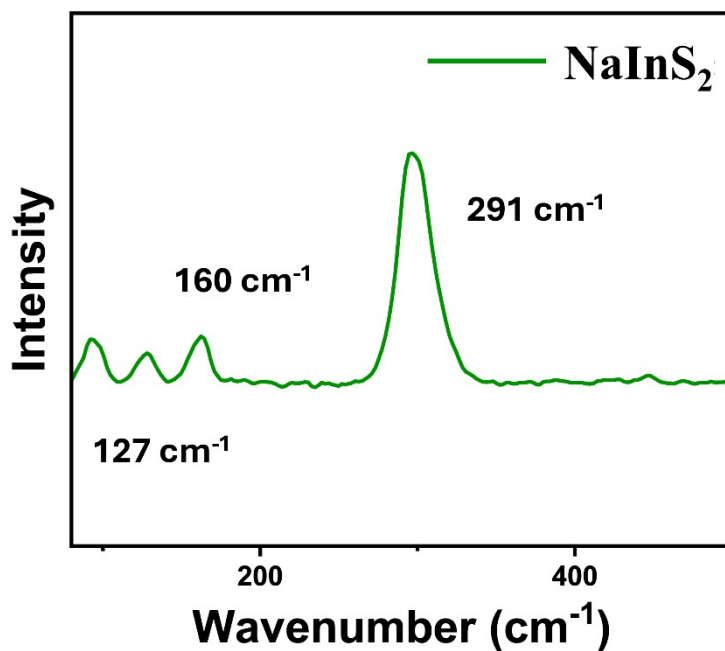


Figure S13 Raman spectra of NaInS₂ NCs.

2.10 XRD, TEM and STEM-EDS analysis for In-S aliquot

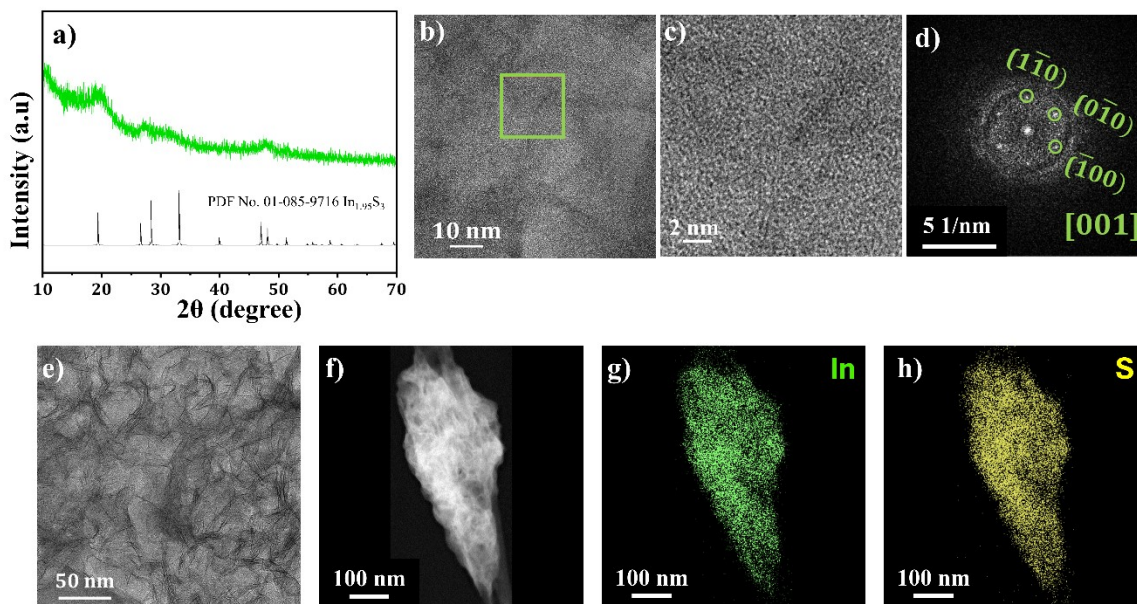


Figure S14 Analysis of In-S template before Na injection a) XRD analysis b) HRTEM of In-S template c-d) an enlarged view of the highlighted area (green square) in (b) and its FFT showing crystallographic orientation and interplanar distances. e) TEM image of In_{1.95}S₃ particles f-h) HAADF image, and corresponding STEM-EDS maps for In and S.

2.11 Control experiments

2.11.1 Temperature variation study

Control experiments were conducted to determine the optimal temperature window for NaInS_2 formation (Figure S14). The phase evolution of Na-In-Se NCs was first examined by XRD as a function of Na-oleate injection temperature. The XRD patterns confirm the formation of NaInS_2 , as the main diffraction peaks match the standard reference pattern NaInS_2 (JCPDS 04-003-9955) for all temperatures from 180-300 °C (Figure S15). At 180 °C, the diffraction peaks are broad and weak, indicating poor crystallinity and incomplete ternary phase transformation. With increasing temperature to 220 °C, the peaks become more visible, suggesting improved crystallization. At 260 °C and 300 °C, the diffraction peaks are sharper and more intense, confirming higher crystallinity and better phase formation. This indicates that elevated temperature promotes atomic diffusion and crystal growth. The TEM images further support this temperature-dependent evolution. At 180 °C, the product mainly consists of In-S binary nanosheets along with few defined nanoplates with weak lattice contrast, indicating incomplete transformation from binary to ternary (Figure S16a-d). Above 220 °C, the TEM images show the clear formation of ternary NaInS_2 NCs, accompanied by improved crystallinity (Figure S16e-l).

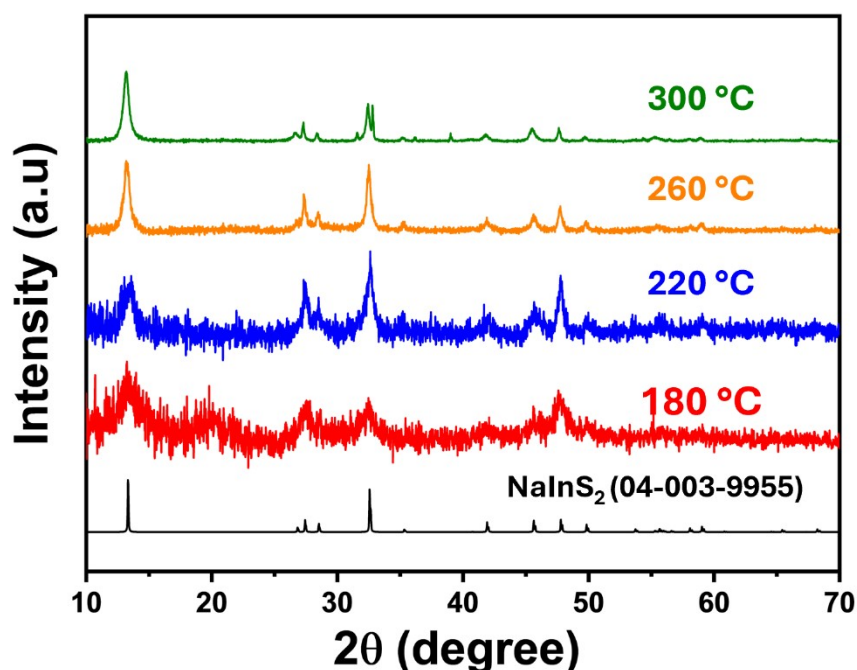


Figure S15 XRD patterns of Na-In-S NCs synthesized by injecting Na-oleate at different temperatures.

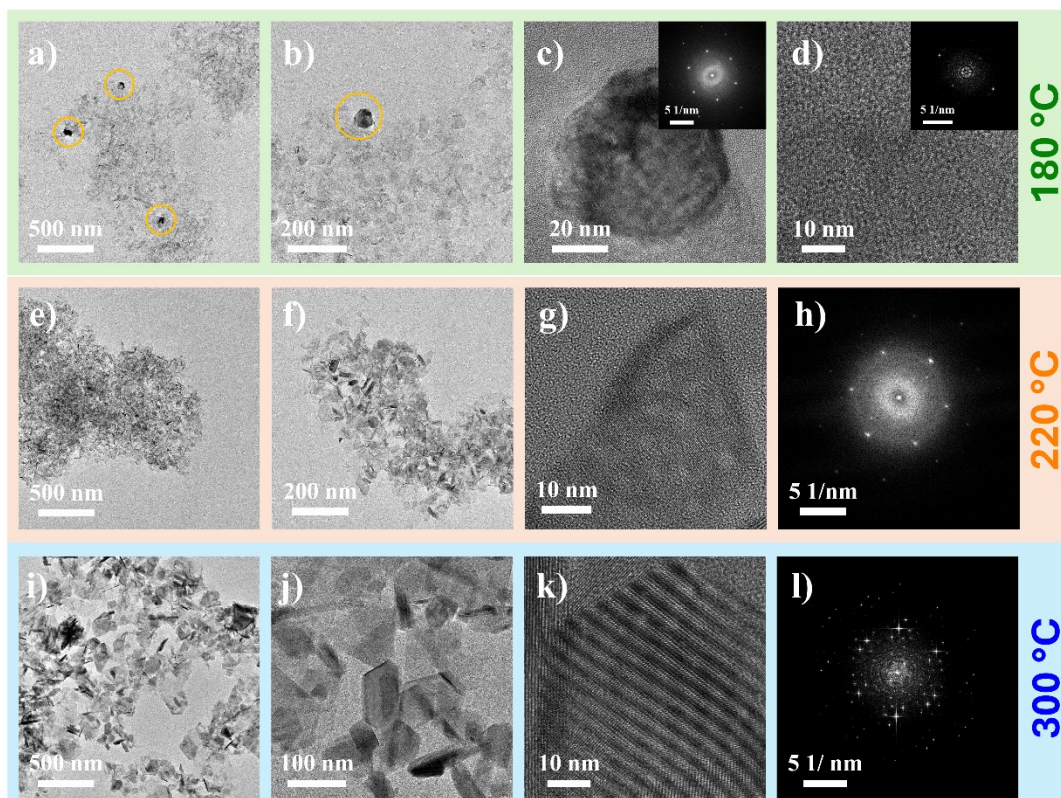


Figure S16 TEM images of Na-In-S NCs synthesized by injecting Na-oleate at different temperatures.

2.11.2 S source variation study

The effect of different sulfur precursors on the formation of NaInS_2 was investigated using 1-DDT, thiourea, and DPDS, and compared with elemental sulfur powder. The XRD patterns show that the products obtained from S powder, 1-DDT, and thiourea mainly match the standard NaInS_2 phase (JCPDS 04-003-9955), confirming successful binary-to-ternary conversion (Figure S17). In these cases, the absence of strong In_2S_3 reflections indicates that the intermediate binary phase is largely consumed during ternary NaInS_2 formation. In contrast, the DPDS-derived sample shows diffraction peaks corresponding to NaInS_2 along with additional features associated with In_2S_3 , indicating incomplete conversion (Figure S17). This suggests that DPDS provides sulfur species more slowly or less effectively under the same reaction conditions, leaving some residual binary In_2S_3 phase.

TEM analysis further confirms the precursor-dependent morphology. The 1-DDT and thiourea samples form aggregated plate-like NaInS_2 NCs with clear lattice fringes and SAED patterns, supporting ternary phase formation (Figure S18a-h). The DPDS sample, however, shows mixed morphologies, including elongated wire-like structures formed by arranged nanoplates and nanoparticles further confirming the incomplete transformation and coexistence of residual In_2S_3 (Figure S18i-l). Overall, these results show that sulfur precursor chemistry strongly affects the binary-to-ternary transformation, with S powder, 1-DDT, and thiourea promoting NaInS_2 formation, while DPDS leads to partial retention of In_2S_3 .

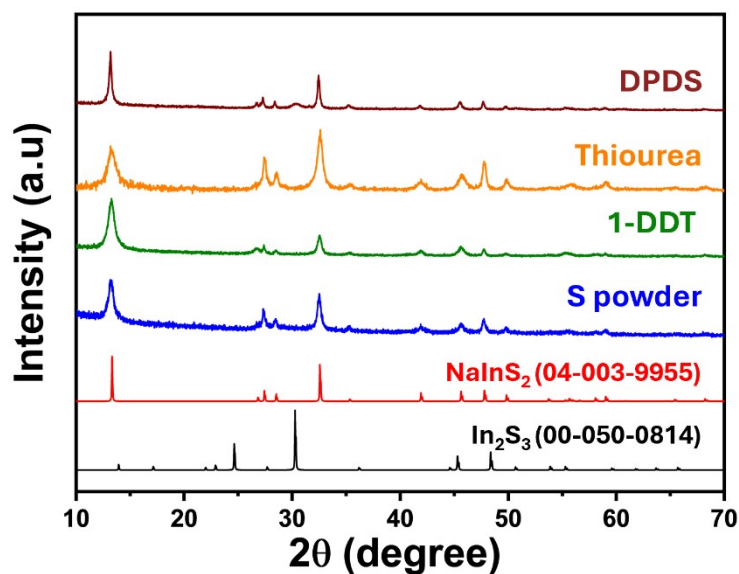


Figure S17 XRD patterns of Na-In-S NCs synthesized by using different S sources.

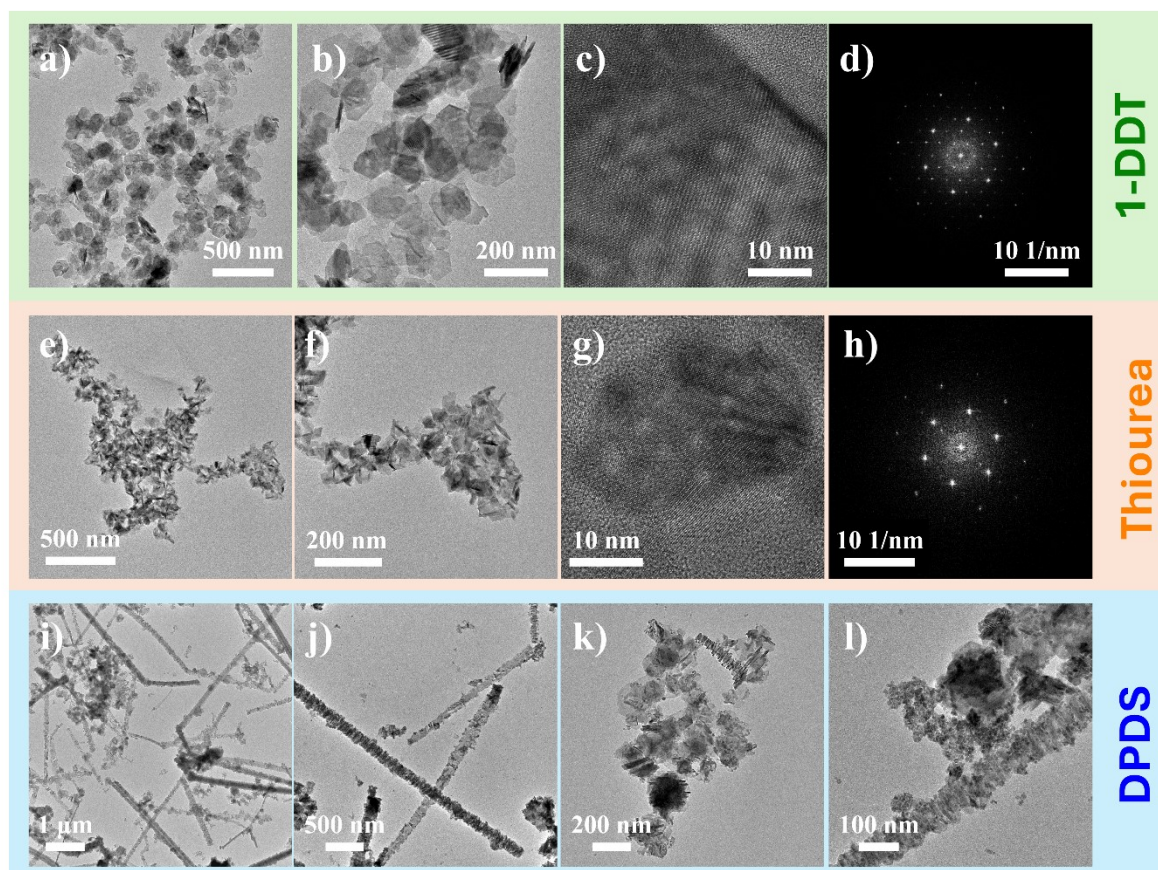


Figure S18 TEM images of Na-In-S NCs synthesized by using different S sources.

2.11.3 Time variation study

The effect of reaction time on NaInS₂ formation was examined at 260 °C by comparing products obtained after 30 min and 60 min (Figure S19a). Although the XRD patterns of the 30 and 60 min samples do not show a significant difference, TEM and STEM images of the 30

min product show nanoplates with nanosheet presence, suggesting that some In-S nanosheets (binary template) are still present at shorter reaction time (Figure S19b-e). This indicates that 30 min is insufficient for complete binary-to-ternary conversion. With longer reaction time, the transformation proceeds further, leading to better-defined and more crystalline NaInS₂ NCs.

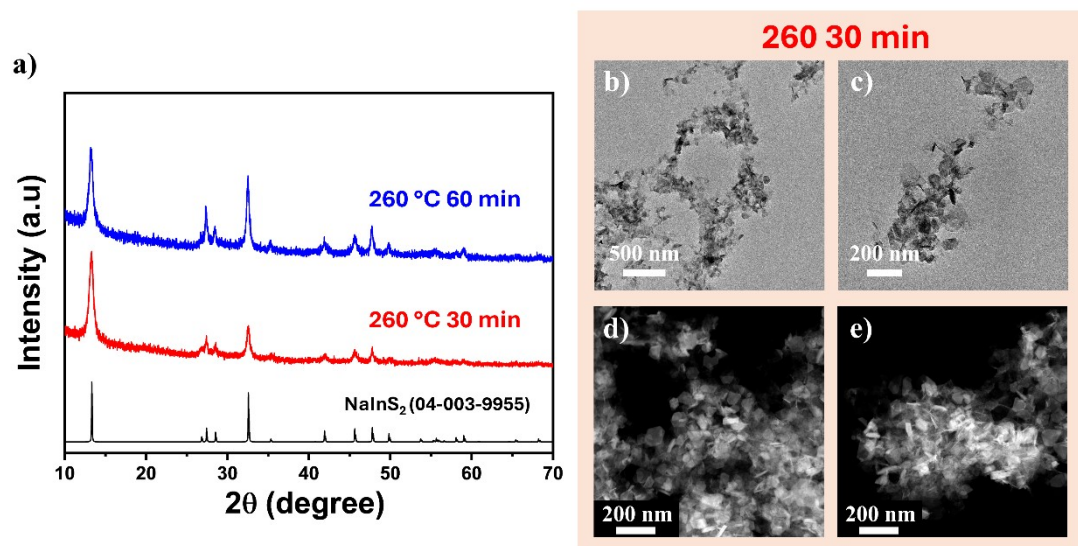


Figure S19 a) XRD pattern and b-e) TEM and STEM images of Na-In-S NCs synthesized at 260 °C with a reaction time of 30 min.